THE ASTROPHYSICAL JOURNAL, 417:565–571, 1993 November 10

POLARIZATION OF THE THERMAL EMISSION FROM THE DUST RING AT THE CENTER OF THE GALAXY

R. H. HILDEBRAND,[1,2,3] J. A. DAVIDSON,[4] J. DOTSON,[1,2] D. F. FIGER,[1,2] G. NOVAK,[5] S. R. PLATT,[5] AND L. TAO[1,3]

Received 1992 July 16; accepted 1993 May 17

ABSTRACT

We present new results on the polarization of the far-infrared emission from the dust ring at the center of the Galaxy. Previous far-infrared polarimetry of the region has been confined to the main ridge of emission. The new measurements cover the entire area of the ring. Polarization maps computed for magnetic fields with biaxial symmetry cannot be made to fit the data. Maps computed for axisymmetric fields provide much better fits, but the results show that the ring and field cannot both have ideal symmetry. The dispersion of the measured position angles about the directions computed from the self-similar model of Wardle & Königl (1990) is comparable to the dispersion about mean values observed in the most orderly dark clouds. The observed polarization is consistent with a model which deviates from axisymmetry by a small distortion of the field or by nonuniform distribution of the emitting dust.

Subject headings: Galaxy: center — infrared: interstellar: continuum — polarization

1. INTRODUCTION

Wherever disks of interstellar material rotate about massive central objects, one may expect that magnetic fields will play a role in constraining outflows, braking rotation, providing support against collapse, or removing angular momentum and aiding accretion. Among all such disks, the only one for which it is now feasible to measure the configuration of the magnetic field is the dust ring discovered by Becklin, Gatley, & Werner (1982) at the center of the Galaxy.

That ring has been studied in detail (Genzel & Townes 1987; Morris 1989). Mid- and far-IR observations of the dust emission show that the ring has an inner radius of ~ 1 pc (for $D = 8$ kpc) and that it surrounds a luminous central source (Becklin et al. 1982; Davidson et al. 1992). Molecular line observations show that the ring is flared and nearly complete, that it rotates about an axis inclined to the line of sight by $i \approx 70°$ (or $i' = 180° - i$), and that the enclosed mass is $\sim 5 \times 10^6\ M_\odot$ (Genzel et al. 1985; Güsten et al. 1987; Jackson et al. 1993).

Information on the magnetic field in and around the ring has been derived from radio continuum measurements, from OH Zeeman measurements, and from near- and far-IR polarimetry. The radio measurements show nonthermal arcs and "threads" near the ring extending tens of parsecs in a direction perpendicular to the plane of the Galaxy. Polarization measurements of the radio emission show that a magnetic field runs along the arcs (see reviews by Yusef-Zadeh 1989 and Morris 1990). Killeen, Lo, & Crutcher (1992) and Schwarz & Lasenby (1990) have reported net fields of the order of -2 mG (toward Earth) in both southern and northern portions of the ring. Aitken et al. (1991) have used polarimetry of the 12.4 μm emission from hot grains in the central ionized cavity to infer a magnetic field running directly along the "northern arm," a feature seen in radiographs (e.g., Lo & Claussen 1983; Killeen & Lo 1989) and in near-IR photometric maps (Becklin et al. 1978). With less regularity, the field runs along the bar that crosses the southern end of the northern arm.

The magnetic structure of the rotating ring has been inferred from 100 μm measurements of the polarization at six points along the central ridge of far-IR emission (Werner et al. 1988; Hildebrand 1989; Hildebrand et al. 1990). Two of the measured points, however, were in a region where the far-IR flux is dominated by the northern arm which is not a component of the ring, and all of the points were in regions where the polarization is nearly uniform. The observations described here have been made with a greatly improved polarimeter. We reexamine the structure of the field on the basis of measurements that cover the entire area of the ring and show considerable variation in the degree and direction of the polarization.

2. OBSERVATIONS

The observations were made from the Kuiper Airborne Observatory during flights on 1991 June 13 and 17. The design and operation of the polarimeter, STOKES, and the techniques used to calibrate the instrument and analyze the data have been described by Platt et al. (1991). After passing through a quartz half-wave plate turned by a stepper motor, the incoming radiation was separated into two orthogonal components of polarization by a free-standing wire grid inclined at 45° to the optic axis. The reflected and transmitted components were detected simultaneously for each pixel on the sky by corresponding pairs of detectors in two 16-detector arrays. The 16 pixels were arranged in a 4×4 array spaced 37".3 center-to-center. Two of the 16 pixels were not in operation.

The nominal beam diameter was 35". The two arrays, however, were not accurately aligned. Because the misalignment involved both translation and rotation, the effective pixel shape varied somewhat over the array with a mean value of $35'' \times 57''$. The pixel positions given in Table 1 and Figure 1 are the average positions of the centers of the corresponding beams. In order to test for possible systematic effects due to the misalignment, we have compared the results for two orientations of the arrays with respect to the sky; one with corre-

[1] Enrico Fermi Institute, University of Chicago, Chicago, IL 60637.
[2] Department of Astronomy and Astrophysics, University of Chicago, Chicago, IL 60637.
[3] Department of Physics, University of Chicago, Chicago, IL 60637.
[4] NASA/Ames Research Center, Moffett Field, CA 94035.
[5] Department of Physics, Princeton University, Princeton, NJ 08544.

TABLE 1

POLARIZATION OF THE 100 μm EMISSION FROM SGR A

YEAR	INSTRUMENT	OFFSET[a]	POLARIZATION		NUMBER OF MEASUREMENTS
			Degree	Angle[b]	
1987[c]	POLY[d]	12″E, 34″N	1.9% ± 0.3%	91° ± 5°	...
		0, 0	1.1 ± 0.3	102 ± 9	...
		18 W, 28 S	0.9 ± 0.3	90 ± 11	...
1988, 1989[e]	POLY[d]	0″, 115″N	2.8% ± 1.4%	73° ± 14°	...
		0, 75 N	2.3 ± 0.4	77 ± 5	...
		12 E, 34 N	2.8 ± 0.3	85 ± 3	...
		0, 0	2.4 ± 0.3	95 ± 3	...
		18 W, 28 S	1.5 ± 0.3	93 ± 5	...
		18 W, 65 S	1.2 ± 0.4	100 ± 8	...
1991	STOKES[f]	56″E, 93″N	1.4% ± 0.3%	71° ± 6°	12
		19 E, 93 N	1.4 ± 0.4	88 ± 8	12
		19 W, 93 N	1.3 ± 0.4	77 ± 8	12
		56 W, 93 N	1.4 ± 0.4	142 ± 9	12
		56 E, 56 N	1.1 ± 0.3	91 ± 7	20
		19 E, 56 N	2.1 ± 0.2	88 ± 3	29
		19 W, 56 N	0.9 ± 0.3	91 ± 8	29
		56 W, 56 N	0.9 ± 0.3	115 ± 8	29
		56 E, 19 N	0.5 ± 0.2	109 ± 13	26
		19 E, 19 N	1.4 ± 0.2	99 ± 5	35
		19 W, 19 N	1.2 ± 0.2	103 ± 5	35
		56 W, 19 N	1.8 ± 0.2	111 ± 3	35
		56 E, 19 S	0.6 ± 0.3	57 ± 12	29
		19 E, 19 S	0.6 ± 0.2	89 ± 12	32
		19 W, 19 S	1.3 ± 0.2	87 ± 5	35
		56 W, 19 S	2.2 ± 0.2	115 ± 3	35
		56 E, 56 S	1.0 ± 0.4	93 ± 10	23
		19 E, 56 S	0.5 ± 0.5	111 ± 28	15
		19 W, 56 S	1.4 ± 0.3	94 ± 6	23
		56 W, 56 S	1.6 ± 0.2	112 ± 4	23
		56 E, 93 S	1.0 ± 0.5	160 ± 16	6
		19 E, 93 S	1.8 ± 0.7	73 ± 12	6
		19 W, 93 S	2.2 ± 0.5	73 ± 7	6
		56 W, 93 S	2.9 ± 0.6	106 ± 6	6

[a] Offsets from $17^h49^m29^s.4$, −28°59′19″ (1950).
[b] Position angle of *E*-vector in degrees east from north.
[c] Data from Werner et al. 1988.
[d] Reference: Novak et al. 1989.
[e] Data from Hildebrand et al. 1990.
[f] Reference: Platt et al. 1991.

sponding beam centers displaced approximately north-south and one with the displacement approximately east-west. For each of the 19 points measured with both orientations, we computed the ratios of the Stokes parameters. The deviations from a ratio of one had reduced χ^2 values $\chi^2(q) = 0.8$ and $\chi^2(u) = 1.1$. We conclude that the misalignment introduced no significant systematic effect except loss of spatial resolution. The effective resolution after combining data for the two orientations was ∼45″ FWHM.

The passband was 80 to 120 μm with a mean wavelength of 100 μm. The chopping direction was approximately perpendicular to the Galactic plane; the amplitude was 7′. Observations of the molecular cloud Sgr B2 (Novak et al. 1993) and of a portion of the arched filaments ∼10′ north of the dust ring (Morris et al. 1992) were made with the same instrument on June 9 and 19. Data from all four flights were used to determine the instrumental polarization. The total flight time during observations of the dust ring was 4 hr 31 minutes. The average flux density at the 17 points for which the signal to noise was greater than 3 was 1300 Jy per 35″ beam. The average flux density in the reference beams was 160 Jy.

3. RESULTS

The results are shown in Table 1 and Figure 1. In the figure the polarization vectors are drawn on a map of the continuum flux at 90 μm (Davidson et al. 1992).

Along the central ridge of emission where the new and the earlier results can be compared, we find good agreement. In that region the polarization vectors are aligned approximately east-west. The new results show a shift in the direction of polarization at the westernmost points by ∼30° counterclockwise, as compared to those along the central ridge and a drop in the degree of polarization in the southeast quadrant. To compare the polarization in the four quadrants, we first discard the points that may be influenced by extraneous clouds (see Fig. 1 and § 5.1) and then combine the remaining points by adding Stokes parameters; that is, we use our data to estimate the polarization to be expected for a single beam covering the area of those points. The results are as follows:

Southeast: (6 points),

$$P = (0.5 \pm 0.2)\%\,, \quad \alpha = (83° \pm 12°)\,.$$

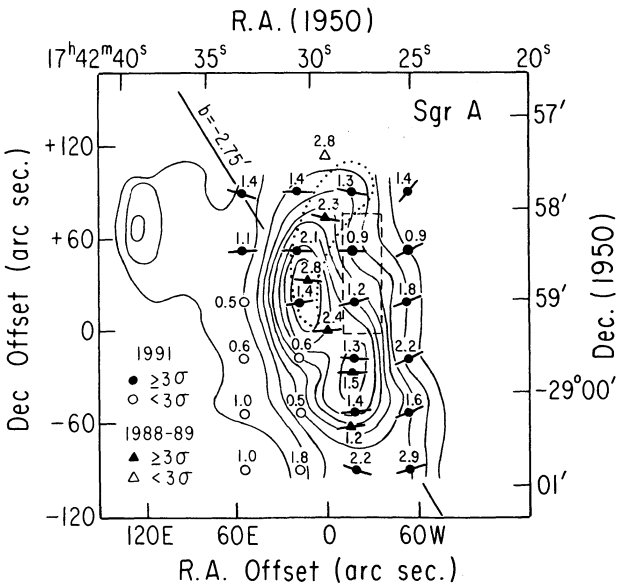

FIG. 1.—Polarization of the far-IR emission from the dust ring at the center of the Galaxy. Vectors showing the direction of the polarization (*E*-vectors) of the new measurements and those from earlier observations (*triangles*) (Hildebrand et al. 1990) are superposed on the 90 μm flux density map of Davidson et al. (1992). Open circles and triangles denote measurements with signal to noise ratio <3. The numbers are the degrees of polarization in percent. Offsets are measured from $17^h42^m29^s.4$, $-28°59'19''$ (1950). Linear scale: 1 pc = 26″ for $D = 8$ kpc. The dotted and dashed lines show approximate outlines of clouds that are not associated with the rotation of the ring. The dotted outline represents the region of far-IR emission associated with the northern arm. The dashed rectangle represents the +70 km s^{-1} feature.

Southwest: (6 points),

$$P = (1.5 \pm 0.2)\%\,, \quad \alpha = (109° \pm 4°)\,.$$

Northwest: (3 points),

$$P = (1.4 \pm 0.2)\%\,, \quad \alpha = (115° \pm 3°)\,.$$

Northeast: (4 points),

$$P = (0.9 \pm 0.2)\%\,, \quad \alpha = (88° \pm 6°)\,.$$

4. RELATIONSHIP BETWEEN POLARIZATION AND FIELD CONFIGURATION

The spin axis of a dust grain becomes aligned or partially aligned with the local magnetic field, ***B***. The long axis of the grain and hence the ***E***-vector of the emitted radiation is perpendicular to the spin axis and thus perpendicular to ***B*** (see review by Hildebrand 1988). For a three-dimensional object such as a ring of appreciable thickness inclined to the line of sight, one cannot derive the configuration of the field from a two-dimensional map of polarization vectors. One must use the map to guess a magnetic model, derive from the model a polarization map convolved with the appropriate beam, compare the derived map with the observed map, and, if necessary, guess again.

For an assumed model, one must add the Stokes parameters I, Q, and U for each volume element along the line of sight, where the intensity I is estimated from the assumed dust density and temperature and where the reduced Stokes parameters, $q = Q/I$ and $u = U/I$, are derived from the assumed direction of the field. An implicit assumption of this procedure is that for the object under investigation, the alignment of the spin axis with the local field ***B*** is independent of $|\boldsymbol{B}|$ (Hildebrand et al. 1990). This assumption is supported by the recent investigations of Jones, Klebe, & Dickey (1992). In most cases, including the Galactic center, no significant correction is required for absorption at 100 μm.

5. DISCUSSION

Before discussing models for the magnetic field, we consider the extent to which the polarized emission could be due to material that is not associated with the rotating ring. We conclude that extraneous clouds may contribute significantly in restricted areas. Excluding those areas, we first compare the observed polarization with predictions based on axisymmetric models of the ring, that is, models in which the rotation of the ring winds up a field initially parallel to the axis of rotation. The resulting field configurations are the simplest from the standpoint of theoretical modeling. In discussing the axisymmetric model giving the best fit to the data, we consider the dispersion in direction to be expected about an idealized field configuration. We next consider biaxial models in which the initial field is perpendicular to the axis. We then consider qualitatively the nature of asymmetric models that could account for the results, and, finally, we comment on models in which the ambient field is neither parallel nor perpendicular to the axis.

5.1. *Source of the Polarized Flux*

Molecular line observations show that in the area of our observations, the preponderance of the molecular emission is from gas in a rotating ring with a sharp inner radius of ~1.5 pc (Güsten et al. 1987; Jackson et al. 1993). Immediately inside this radius, radio continuum and [Ne II] observations (e.g., Lo & Claussen 1983; Serabyn et al. 1986) show ionized arcs or streamers. The position and velocity of one of these features, the western arc, imply that it is the ionized inner edge of the molecular ring. Another arc, the "northern arm," is not connected with the ring; it is apparently a stream of material falling into the central cavity from a region at least 3 pc north of the center (Jackson et al. 1993). An analysis by one of us (J. A. D.) has shown that the maps of far-infrared emission (Davidson et al. 1992) cannot be fitted assuming emission only from a ring of inner radius 1.5 pc supplemented by emission from the northern arm: the effective inner radius for dust emission must be 0.5–1.0 pc.

The recent observations of Jackson et al. (1993) show that the atomic [O I] line is associated with the arcs in the cavity rather than the molecular ring, and the velocities given by the atomic line are consistent with those of the ionized arcs. The [O I] and continuum measurements indicate that the "ionized arcs" within the cavity are, in fact, predominantly neutral. The material associated with the western arc probably represents the atomic and ionized portion of the circumnuclear ring which is interior to the molecular portion of this ring. Thus, except in the vicinity of the northern arm, the brightest parts of the far-IR map are due to emission from a region of inner radius ~1 pc composed of ionized and atomic material that rotates with the ring. The regions of lower flux density at $r > 1.5$ pc are associated with the molecular portion of the ring.

The far-IR emission from the region enclosed by the dotted line in Figure 1 appears to be associated primarily with the northern arm and not with the material in the rotating ring. The radio continuum from the northern arm is especially bright in the portion within ~1 pc of the center but can also be

seen at larger radii (e.g., Brown & Liszt 1984; Zylka & Mezger). The 1300 μm (Mezger et al. 1989) and far-IR (Davidson et al. 1992) flux density maps show ridges of emission extending along the entire length of the "dotted" region (see Fig. 1 and the 50 μm map of Davidson et al. 1992; [their Fig. 4]). The ridge of atomic [O I] emission, extending out to $\sim$3 pc, bends to the right somewhat more than the broader ridges of continuum emission.

Other regions showing emission that is not associated with the rotating ring have been identified by Güsten et al. 1987; Ho et al. 1985; Genzel et al. 1990; Zylka, Mezger, & Wink 1990; Jackson et al. 1993. Among these the only one that has a sufficient column density of warm dust to contribute significantly to the 100 μm continuum is the "+70 km s^{-1} feature" $\sim$10″–30″ west of Sgr A*. The region occupied by that feature is shown approximately by the dashed rectangle in Figure 1. We shall exclude both the region of the northern arm and the region of the "70 km s^{-1} feature" when comparing our data with the predictions of models for the rotating ring.

5.2. *The Magnetic Field in the Ring*

We now consider the constraints that are imposed by our data on models for the magnetic field in the ring.

5.2.1. *Models with Axisymmetry*

Wardle & Königl (1990) have proposed an axisymmetric model for the magnetic field in the dust ring. They assume that a field parallel to the axis is drawn inward by accretion and in the φ-direction by differential rotation (Fig. 2*a*). The advection and shearing of the field are balanced by ambipolar diffusion. This is a modified version of the self-similar model proposed earlier by Königl (1989) but with Keplerian velocities replaced by a constant velocity and with corresponding changes in the r-dependence of the radial velocity, the density, the ion density, and the magnetic field intensity: for the new model, v_r = const, $\rho \propto r^{-2}$, $\rho_i \propto r^{-1}$, and $\boldsymbol{B} \propto r^{-1}$. The polarization predicted by the model does not depend strongly on these relationships. As in any self-similar model, the thickness of the ring is proportional to r. The model permits a wide range of choices for the field configuration.

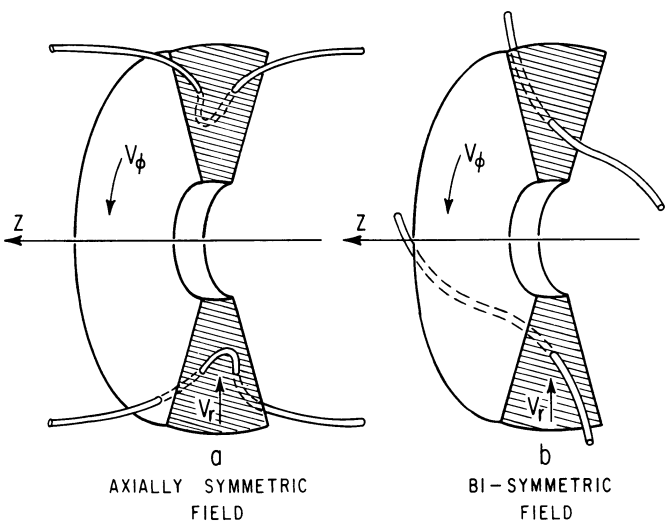

FIG. 2.—Cross section of an idealized accretion disk. The magnetic field is represented schematically by two flux tubes for each of two models for the magnetic field: (*a*), one, axisymmetric and another, (*b*), bi-symmetric. The disk is shown in the orientation inferred from this work and from other observational data (north up, ring highly inclined, west side is near, north end is receding).

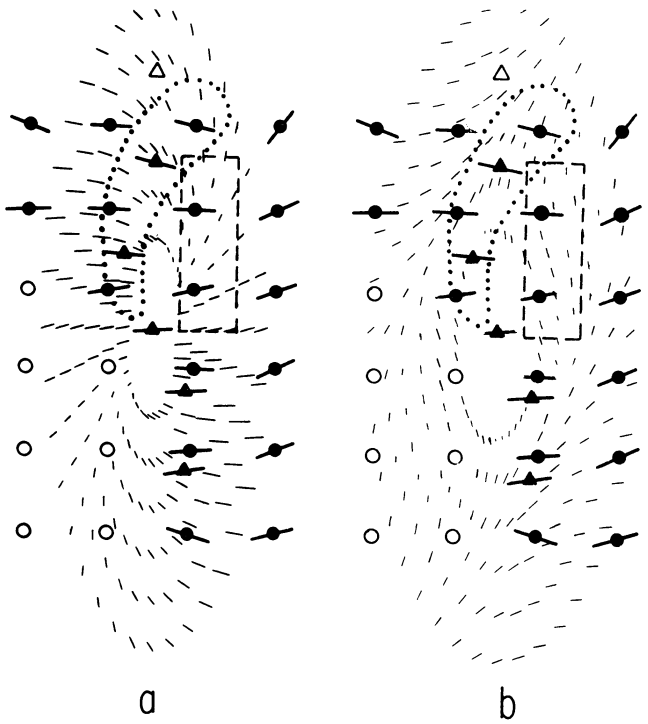

FIG. 3.—Comparison of the measured polarization with the maps computed for (*a*) axisymmetric and (*b*) bisymmetric fields. (Symbols as defined in Fig. 1.) The axisymmetric map is drawn for the model shown in Fig. 4. It can be extended keeping the polarization uniform along any given radial line.

We shall assume, initially, that at the Galactic center the ring axis and the ambient field are aligned well enough that such a model can be applied.

In Figure 3*a* we compare our results with the pattern of polarization derived by Wardle & Königl (1990) for their model "gc2" (Fig. 4). The inclination to the line of sight is 70°, and the major axis of the projected ring is at 0° (N-S). We can

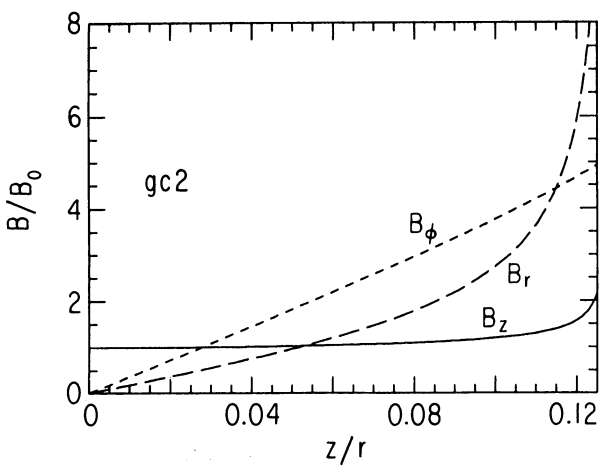

FIG. 4.—Components of the field in a magnetic accretion disk: one of five examples (example gc2) given by Wardle & Königl (1990). The relative magnitudes of the z, r, and φ components are shown as a function of z/r, where z is the distance from the median plane at an arbitrary radius, r. The surface of the disk is assumed to be at $z/r \approx 0.125$.

conveniently extend the comparison to the other examples given by Wardle & Königl (1990) by employing a property inherent in self-similar models: the polarization is independent of radius. If we assume that the ring is uniform and symmetric and consider only points that are beyond the surface of the central cavity, then the direction of polarization, α, predicted by the model should be the same for all points along a given radial line and the same for all points at θ and at $\theta + \pi$. In Figure 5 we show values of α versus θ, where θ is the polar angle measured from the long axis (in this case, north). The points are all those of $\geq 3\,\sigma$ significance which are outside the areas with known external clouds (Figs. 1 and 3). The curves are drawn for the five field configurations presented by Wardle & Königl (1990). These can be approximately described as follows.

gc1—Same as Figure 4 except B_r doubled.

gc2—Figure 4.

gc3—Same as Figure 4 except $B\varphi$ reduced to $\sim 2B_0$ at surface. ($B_0 = B$ at $z = 0$).

gc4—Same as Figure 4 except B_r reduced everywhere below B_z.

gc5—$B\varphi$ reduced to $\sim 2B_0$ at the surface; B_r reduced everywhere below B_z.

For all the models $B_z/B_0 \approx 1$ everywhere except near the surface.

As is evident in Figure 5, models gc3, gc4, and gc5 are all inconsistent with the data. Moreover, these configurations would, in contrast to the data, give higher polarization in the southeast than in the southwest quadrant. The bottom curve, gc1′, shows the polarization to be expected for the field configuration, gc1, of Figure 4 if, instead of an inclination $i = 70°$ (rotation counterclockwise: near side is west), we assume an inclination $i' = (180° - 70°) = 110°$ [rotation clockwise: near side is east; $\alpha'(\theta) = \pi - \alpha(\pi - \theta)$]. Evidently, we can exclude both $i' \approx 110°$ and any model in which the azimuthal and radial components of the field are not much greater than the axial component at the surface of the disk.

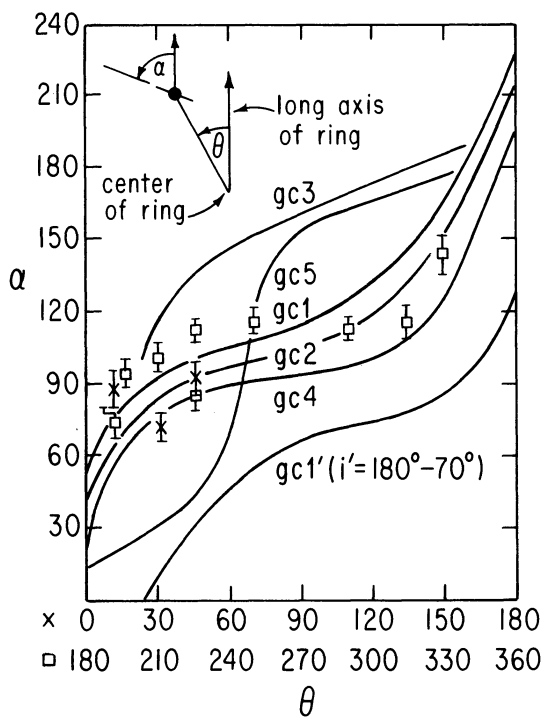

FIG. 5.—Comparison of the measured polarization angles with angles predicted for the self-similar models computed by Wardle & Königl (1990). The field configurations gc1–gc5 are described in § 5.2.1. The ordinate, α, is the position angle of the polarization (*E*-vector measured east from north) at a point with polar coordinates (θ, r) in the plane of the sky. For self-similar models, α is independent of r. For the curves gc1–gc5, the axis of rotation of the ring is assumed to be at an inclination $i = 70°$ (rotation counterclockwise; west side near). For the curve gc1′ (*bottom curve*), the axis is assumed to be at $i' = (180 - 70)°$ (clockwise; east side near). Crosses denote measurements at points $0 < \theta < 180°$; squares denote $180° < \theta < 360°$.

The curve, gc2 (Fig. 5) giving the best fit to the new measurements is similar to the curve for gc1, the model tentatively selected on the basis of the earlier measurements (Hildebrand et al. 1990). However, the near agreement in the choice of models is, in part, fortuitous. Two of the original six points were within the lower portion of the northern arm, where the direction of the field measured by Aitken et al. (1991) is nearly the same as that predicted by the model. As discussed in § 5.1, we now exclude the entire area of the northern arm when fitting models for the ring.

One cannot expect the polarization observed in a ring that is clumpy, turbulent, and possibly warped to follow exactly the predictions of an idealized model. Nor can one expect a self-similar model with a sharp upper bound for $|z/r|$ and no upper bound for r to be entirely satisfactory, even as an ideal. The dispersion of the measured polarization angles about the predicted values for the model gc2 (Fig. 5) is 14° rms. The median dispersion is 9°. There are no objects of comparable turbulence for which one can compare data on polarization with predicted maps. The only available comparisons are with dispersions about mean values in less turbulent sources. In Orion the dispersion of the eight measured values of far-IR polarization is 12° rms. (Gonatas et al. 1990). In optical observations of the most orderly dark clouds Myers & Goodman (1991) find distributions of polarization with median dispersions of 0.2–0.4 radians (11°.5–23°). In dark clouds with embedded clusters they find median dispersions of 0.4–0.5 radians (23°–29°). To the extent that they are relevant, these comparisons support the conclusion that the axial field gc2 fits the data on position angles as well as could be expected. A comparable fit could be obtained if the axis of rotation as projected on the sky were shifted from 90° (east of north) to as much as 115°.

One cannot conclude, however, that a model with perfect axisymmetry gives a satisfactory fit to the data. For perfect axisymmetry the polarization should be the same in the southeast and northwest quadrants.

5.2.2. *Bisymmetric Models*

We have assumed an axisymmetric field—or at least an ambient field more nearly parallel than perpendicular to the axis—on the basis of the long nonthermal arcs that cross the Galactic plane at 90° near Sgr A (Morris & Yusef-Zadeh 1989). In the thermal filaments, however, just south of the arcs and only $\sim 10'$ north of the ring, we find a field in the orthogonal direction, i.e., approximately parallel to the plane of the Galaxy and much closer to the plane of the disk than to the axis (Morris et al. 1992). It is therefore appropriate to consider whether the field may have a "biaxial" configuration: that is, the configuration that would be produced if flux tubes in the plane of the ring were bent into S-shapes by the rotation (Fig. 2*b*). The general characteristics of such fields have been discussed by Parker (1979).

It is possible for a bisymmetric field in an inclined ring to

reproduce some of the qualitative features of an axisymmetric field. For example, the quadrants showing the lowest degrees of polarization can be the same, and, in either case, $\alpha(\theta, r) = \alpha(\theta + \pi, r)$. Other features, however, will be markedly different. For axial symmetry, $d\alpha/d\theta$ is positive, everywhere, and $d\alpha/dr|_\theta = 0$. For biaxial symmetry $d\alpha/d\theta$ changes sign four times between $\theta = 0°$ and $\theta = 2\pi$ and $d\alpha/dr|_\theta \neq 0$: the field is increasingly twisted as r decreases (Figs. 3*b* and 6). Our measurements show neither of the latter characteristics.

In Figure 6 we compare our results with curves computed for a bisymmetric model at each of several radii. The curves are drawn for the same conditions, except field direction, as used for the axial model. The shearing of the field is balanced by ambipolar diffusion. The measurements do not show the radial dependence computed for the model and do not fit the computed curves at any radius. The predicted range of values of $\alpha(\theta)$ depends on the assumed conditions, but we find no conditions for which the predictions give a satisfactory fit to the data.

5.2.3. *Asymmetric Models*

We have shown that bisymmetric models are altogether unsatisfactory and that axisymmetric models, though in much better agreement with the results presented here, do not explain the observed asymmetry with respect to reflection through the origin. That asymmetry, however, can easily be produced by a distortion of the field or an asymmetric distribution of material in the ring.

The HCN observations of Jackson et al. (1993) show that there is no significant warp of the plane of the ring at $r \approx 2$ pc. At larger radii there could be a warp of the plane or a distortion of the ring such that the position angle of the major axis as projected on the sky shifts with radius. Güsten et al. (1987) find a shift from $\sim 27°$ (east from north) at 2 pc to $\sim 12°$ at 5 pc. That shift, which appears also in the far-IR map of Davidson et al. (1992), may be an effect of the northern arm.

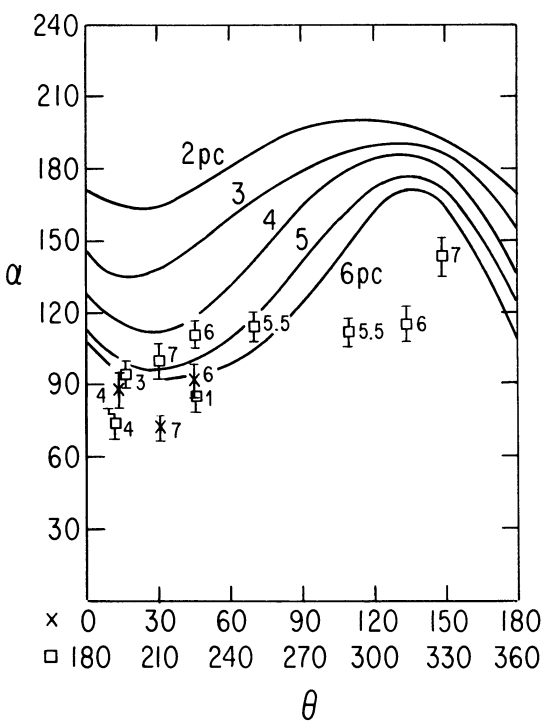

FIG. 6.—Comparison of the measured polarization angles with angles predicted for a bisymmetric model. (Symbols as defined in Fig. 5). The curves give predicted values of $\alpha(\theta, r)$ for radii, r, from 2 pc to 6 pc. Approximate values of r, again in parsecs, are shown for each measured point.

Even if the magnetic field in the disk has perfect axisymmetry, one could nevertheless find an asymmetry in the degree and direction of the polarization, if the material of the ring is not symmetrically distributed. If, for example, the dust in the southeast quadrant is displaced in the $-z$ direction from the median plane of the field, then the degree of polarization in that quadrant will be reduced: in that quadrant, the field at $-z$ is more nearly along the line of sight than at $+z$ (see Fig. 2*a*).

Assuming a field given to first approximation by the axial model, we conclude that the observed asymmetry could plausibly be due to a displacement of emitting dust in an otherwise symmetrical disk.

5.2.4. *Models with Skewed Fields*

The ambient field of the ring is probably neither parallel to the axis of rotation, as assumed for an axisymmetric model, nor perpendicular to the axis as assumed for a bisymmetric model. If, for example, the ambient field is perpendicular to the Galactic plane, as one would infer from the nonthermal arcs to the north, and if the axis of rotation is oriented approximately as described in § 5.2.1, then the field may be $\sim 35°$ from the axis.

From qualitative modeling of the ring, one can deduce that even if the ambient field is skewed as much as $\sim 35°$ from the axis, the rotation should constrain the field within the ring to a configuration that to first approximation is axisymmetric. The relationship $\boldsymbol{B}(r, \theta, +z) = \boldsymbol{B}(r, \theta + \pi, -z)$, which holds for both axisymmetric and bisymmetric models, will still hold if the ambient field is skewed: if there is no gradient or only a radial gradient in the ambient field, then that field will obey the same relationship. Accordingly, one cannot invoke a skewed field to explain asymmetric polarization.

7. SUMMARY AND CONCLUSIONS

We have measured the polarization of the far-IR thermal emission from the dust ring at the center of the Galaxy. The measurements are distributed over the whole area of the ring. Prominent features of the new measurements are a drop in the degree of polarization in the southeast quadrant below the values for the other quadrants and a shift of $\sim 30°$ in the position angles at the six westernmost points.

Molecular and atomic line observations have identified two regions within the mapped area where extraneous clouds may contribute significantly to the far-IR flux. In the remaining area the preponderance of the continuum emission is from dust in the circumnuclear ring. For comparisons of the measured polarization with maps derived from specific models of the magnetic field, we omit points within the boundaries of the extraneous clouds.

Our conclusions are as follows.

1. No bisymmetric model (i.e., no model for which the ambient field is in the plane of the disk) can fit the data.

2. An axisymmetric model can fit the data much better than a biaxial model but cannot account for the observation of differing degrees of polarization in opposite quadrants. (Bisymmetric and axisymmetric models are both invariant with respect to reflection through the origin.)

3. The observed asymmetry in the polarization could be produced in a ring that deviates from axial symmetry because

the ring and the field within the ring are distorted or because the emitting dust is displaced from the median plane in an otherwise symmetrical disk. Such a displacement would alter both the degree and the direction of the polarization. The asymmetry would not be produced by inclination of the ambient field from the axis of the ring.

4. The axisymmetric model giving the best fit to the new data is model gc2 of Wardle & Königl (1990). (The earlier selection [Hildebrand et al. 1990] of model, gc1, giving almost as good a fit, was, in part, fortuitous: two of the points fell in an area where the flux from the northern arm is polarized in the same direction as that given by the model for the ring.) A comparable fit is obtained if the projected angle of the ring axis is shifted from 90° to as much as 115° (east from north).

5. The dispersion of the measured position angles about the values predicted by Wardle & Königl (1990) (for gc2, Fig. 4) is no greater than the dispersion about mean values of the polarization observed by Myers & Goodman (1991) in the most orderly dark clouds.

6. If we assume an axisymmetric model given approximately by gc2 but with some asymmetry as discussed in § 5.2.3, then we confirm the earlier conclusions that the rotation is counter clockwise as projected on the sky and that $B_r \gg B_z$ and $B\varphi \gg B_z$ at the surface of the disk. For field strengths of order 1 mG (inferred from the Zeeman measurements) and for $|B_r|$ and $|B\varphi|$ greater than $|B_z|$, the field may contribute significantly to the vertical compression of the disk (Wardle & Königl 1990). The inequality $B_r \gg B_z$ at the surface of the disk satisfies the condition for centrifugal removal of surface material and hence for removal of angular momentum (Blandford & Payne 1982; Wardle & Königl 1990).

7. A severe test of the model described above can, in principle, be provided by Zeeman or Faraday rotation measurements showing whether the component of the field along the line of sight reverses sign between adjacent quadrants (e.g., the southeast and southwest quadrants) as predicted. Additional tests can be provided by measuring the polarization of the far-IR emission from the ring with better accuracy, better spatial resolution, and more complete sampling and by measuring the direction of the field in regions immediately surrounding the ring, for example, by submillimeter polarimetry sensitive to cooler outlying dust.

We thank the crew of the Kuiper Airborne Observatory for their assistance during the flights. It is a pleasure to acknowledge extensive discussions with A. Königl, R. Rosner, and M. Wardle and other valuable discussions with D. T. Jaffe, M. Morris, E. Parker, C. Townes, and F. Yusef-Zadeh, We thank R. Pernic for his work as project engineer for STOKES and for his participation in the KAO flights. We thank M. Wardle for qualitative modeling of the effects of off-axis fields. We are grateful to the referee for important criticisms of the original manuscript.

The observations were supported by NASA grant NSG-2057. The construction of the instrument was supported by NASA grant NSG-2057 and by NSF grant AST 85-13974.

REFERENCES

Aitken, D. K., Gezari, D., Smith, C. H., McCaughrean, M., & Roche, P. F. 1991, ApJ, 380, 419
Becklin, E. E., Gatley, I., & Werner, M. W. 1982, ApJ, 258, 135
Becklin, E. E., Matthews, K., Neugebauer, G., & Willner, S. P. 1978, ApJ, 220, 831
Blandford, R. D., & Payne, D. G. 1982, MNRAS, 199, 883
Brown, R. L., & Liszt, H. S. 1984, ARA&A, 22, 223
Davidson, J. A., Werner, M. W., Wu, X., Lester, D. F., Harvey, P. M., Joy, M., & Morris, M. 1992, ApJ, 387, 189
Genzel, R., Stacey, G. J., Harris, A. I., Townes, C. H., Geis, N., Graf, U. U., Poglitch, A., & Stutzki, J. 1990, ApJ, 356, 60
Genzel, R., & Townes, C. H. 1987, ARA&A, 25, 377
Genzel, R., Watson, D. M., Crawford, M. K., & Townes, C. H. 1985, ApJ, 297, 766
Gontas, D. P., et al. 1990, ApJ, 357, 132
Güsten, R., Genzel, R., Wright, M. C. H., Jaffe, D. T., Stutzki, J., & Harris, A. I. 1987, ApJ, 318, 124
Hildebrand, R. H. 1988, QJRAS, 29, 327
———. 1989, in IAU Symp. 135, Interstellar Dust, ed. L. J. Allamandola & A. G. G. M. Tielens (Dordrecht: Kluwer), 275
Hildebrand, R. H., Gonatas, D. P., Platt, S. R., Wu, X. D., Davidson, J. A., Werner, M. W., Novak, G., & Morris, M. 1990, ApJ, 362, 114
Ho, P. T. P., Jackson, J. M., Barrett, A. H., & Armstrong, J. T. 1985, ApJ, 288, 575
Jackson, J. M., Geis, N., Genzel, R., Harris, A. I., Madden, S., Poglitsch, A., Stacey, G. J., & Townes, C. H. 1993, ApJ, 402, 173
Jones, T. J., Klebe, D., & Dickey, J. M. 1992, ApJ, 389, 602
Killeen, N. E. B., & Lo, K. Y. 1989, in IAU Symp. 136, The Center of the Galaxy, ed. M. Morris (Dordrecht: Kluwer), 453
Killeen, N. E. B., Lo, K. Y., & Crutcher, R. 1992, ApJ, 385, 585
Königl, A. 1989, ApJ, 342, 208
Lo, K. Y., & Claussen, M. J. 1983, Nature, 306, 647
Mezger, P. G., Zylka, R., Salter, C. J., Wink, J. E., Chini, R., Kreysa, E., & Tufts, R. 1989, A&A, 209, 337
Morris, M., ed. 1989, IAU Symp. 136, The Center of the Galaxy, ed. M. Morris (Dordrecht: Kluwer)
Morris, M. 1990, in IAU Symp. 140, Galactic and Intergalactic Magnetic Fields, ed. R. Beck, P. Kronberg, & R. Wielebeinski (Dordrecht: Kluwer), 361
Morris, M., Davidson, J. A., Werner, M., Dotson, J., Figer, D. F., Hildebrand, R. H., Novak, G., & Platt, S. R. 1992, ApJ, 399, L63
Morris, M., & Yusef-Zadeh, F. 1989, ApJ, 343, 703
Myers, P. C., & Goodman, A. A. 1991, ApJ, 373, 509
Novak, G., Platt, S. R., Goldsmith, P., Davidson, J. A., Dotson, J., Figer, D. F., & Hildebrand, R. H. 1993, in preparation
Parker, E. N. 1979, Cosmical Magnetic Fields: Their Origin and Their Activity (Oxford: Clarendon Press)
Platt, S. R., Hildebrand, R. H., Pernic, R. J., Davidson, J. A., & Novak, G. 1991, PASP, 103, 1193
Schwarz, U. J., & Lasenby, J. 1990, in IAU Symp. 140, Galactic and Intergalactic Magnetic Fields, ed. R. Beck, P. Kronberg, & R. Wielebinski (Dordrecht: Kluwer), 383
Serabyn, E., Güsten, R., Walmsley, C. M., Wink, J. E., & Zylka, R. 1986, A&A, 169, 85
Wardle, M., & Königl, A. 1990, ApJ, 362, 120
Werner, M. W., Davidson, J. A., Morris, M., Novak, G., Platt, S. R., & Hildebrand, R. H. 1988, ApJ, 388, 734
Yusef-Zadeh, F. 1989, in IAU Symp. 136, The Center of the Galaxy, ed. M. Morris (Dordrecht: Kluwer), 243
Zylka, R., & Mezger, P. G. 1988, A&A, 190, L25
Zylka, R., Mezger, P. G., & Wink, J. 1990, A&A, 234, 133